

COMPRESSOR FOULING DETECTION BY IMAGE ANALYSIS

Alessio Suman
Department of Engineering
University of Ferrara, Ferrara,
IT 44122

Nicola Zanini
Department of Engineering
University of Ferrara, Ferrara,
IT 44122

Michele Pinelli
Department of Engineering
University of Ferrara, Ferrara,
IT 44122

ABSTRACT

Gas turbine fouling is commonly known as responsible for performance degradation in terms of compression ratio and efficiency. Fouling is promoted by the adhesion of airborne contaminants coming from natural or artificial sources. Natural contaminants are soil, pollen, or salt, while synthetic contaminants are usually generated by combustion processes such as soot powder. The adhesion of these micro-sized particles caused the modification of the blade shapes and the surface roughness. Both of these two effects determine the modification of the compressor performance over the unit operation.

During overhaul or off-line washing, the deposits on the compressor's internal surfaces are removed, restoring the original performance. However, both land-based units and aero-engines collect several micron-sized particles (soil and soot), which are able to stick to the blade surface depending on the engine load and environmental conditions. Due to the lack of capability to forecast the fouling intensity, it could be useful to estimate the fouling intensity during the machine overhaul, collecting strategical data by which a specific characterization of a given machine in a given operating site can be done. The present paper proposes and validates a helpful methodology for estimating the deposit intensity by an image analysis procedure. An image-detection technique has been carried out before and after the contamination process, and, using a subtraction process, a quantitative analysis of the fouled regions can be developed. Furthermore, image detection has been compared to the localized quantification of the deposits by means of a dust collector.

The results show that, with a careful light and camera setup, the intensity of the deposits can be estimated with an acceptable tolerance band, which allows the possibility of collecting quantitative data on compressor deposits during overhaul operations. This generates a valuable starting point for predicting the overtime degradation of the unit and/or estimating the filtration section efficiency.

NOMENCLATURE

d	particle diameter
N	particle count
S	Stage
mean	mass-averaged diameter

ARD M	Arizona Road Dust Medium
ARD N	Arizona Road Dust Nominal
ARD UF	Arizona Road Dust UltraFine
LAPO	Localized Aspirator for Particle Observation
SEM	Scanning Electron Microscope
SFS	Shape From Shading

INTRODUCTION

Even more constraints related to energy consumption and emission put attention on every energy transformation and consumption. The straightforward way to reduce energy consumption is to increase the efficiency of the devices and systems. In light of this new technology era, gas turbines represent such systems able to easily convert energy in a very small footprint area, making these engines useful for the energy transition process [1, 2].

The gas turbine technology has been developed to increase its efficiency using new technology and design by incrementing the firing temperature and aerodynamic performance and decreasing emissions and fuel consumption. However, gas turbines experience performance degradation during operation due to flow path contamination [3, 4]. This effect is generated by the adhesion of micro-sized particles from fuel and/or the environment [5, 6]. The contamination provided by the fuel impurity affects the turbine section (hot section of the gas turbine, after the combustor), and it can be slowed down by adopting cleaner fuel. By contrast, the contamination provided by the airborne contaminant can be slowed down by inlet filtering sections, but in several applications, the filtration efficiency or the impossibility of using such systems (for example, the aero-engines) determines the compressor section contamination [5].

The contamination is due to the adhesion of such micro-sized particles to the blade and vane surface, generating the gas turbine fouling phenomenon. In addition, this adherent layer determines the modification of the blade shape (especially the leading edge) and the modification of the surface roughness. These effects change the machine compressor performance over the operation time [7, 8]. To slow down these effects, the engine was washed frequently [9, 10] during the operation, even if the performance restoration can be achieved

by employing an off-line washing procedure or machine overhaul [11 – 13].

The root cause of the gas turbine fouling is not straightforward. The adhesion of the contaminant depends on blade/vane surface characteristics (the presence of coating and the surface roughness), the environmental condition (in particular, the relative humidity), and the operating point of the unit. Therefore, the adhesion results from several conditions and the effects on the unit performance. As reported in [14], for the same operating condition, two units could experience different adhesion patterns, and for the same adhesion pattern, two units could experience two different performance degradations (i.e., the machine susceptibility and sensitivity to fouling).

Aim of the work. A detailed investigation of the fouling phenomenon in terms of the adhesion process has to consider the location and intensity of the deposits. This work proposed a new methodology based on image analysis able to detect the deposits over the compressor flow path that could be adopted for lab-scale tests and during the overhaul operation. The proposed methodology is carried out on an actual engine after a controlled contamination process. The novelty of this approach is mainly due to its wide range of applicability. Pros, cons, and guidelines are also highlighted.

MATERIALS AND METHODS

A specific test bench has been set up to test the image detection of fouled compressor regions. The experimental rig was equipped with the compressor of the engine Allison 250 C18. This is a multistage axial unit coupled with a centrifugal stage able to reach an overall pressure ratio of 6.2 and a mass flow rate of 1.36 kg/s at the design speed of 51,600 rpm [15]. The centrifugal stage has two semivolutes, each with a circular exit duct with a diameter of 0.056 m. Two flexible tubes link the outlet ducts to an exhaust outlet with a diameter of 0.100 m. The compressor is driven by an electric motor. During

the current test campaign, the compressor unit has been kept at 20,000 rpm, corresponding to 0.33 kg/s.

According to Fig. 1, the test bench is equipped with an external air treatment section, which allows the setup of the relative humidity at the compressor inlet, and a contaminant injection system, able to disperse micro-sized particles in the airflow swallowed by the unit. The particle feeder is the TOPAS SAG40U, able to prepare and inject the solid contaminants with two Venturi eductors, guaranteeing the proper particle injection process. The contaminants were dosed using a variable-speed rotating ring to increase or decrease the mass per unit of time prepared for Venturi's sucking process. The dosing system and the setup of the contaminant injection are described in [16].

Contaminants. To explore the fouling phenomenon, three powder samples have been considered. In line with the on-field experiences [3], soil particles come from several sources and have different diameters. In particular, the dust carried by the wind covers thousand of kilometers and it is usually characterized by a diameter lower or almost equal to 1 μm . At the same time, bigger soil particles are typically carried by storms for a few kilometers [17, 18]. Therefore, three diameter distributions have been considered to explore the most comprehensive possibility. All of the soil samples are the Arizona Road Dust (ARD) sample, characterized by a density of 2717 kg/m^3 . It is a natural-based powder consisting mainly of about 70 wt. % silica and 14 wt. % aluminum oxide and other minor iron, sodium, calcium, and magnesium oxides. To measure the diameters distribution, the Malvern Microsizer 3000 has been used. The particle diameter distributions for the three powder sample named ARD N ($d_{\text{mean}} = 1.3 \mu\text{m}$), ARD UF ($d_{\text{mean}} = 4.8 \mu\text{m}$), and ARD M ($d_{\text{mean}} = 25.5 \mu\text{m}$) are reported in Fig. 2. In Fig. 2, SEM (Scanning Electron Microscope) detections are reported. Looking at the detections, the soil particles are characterized by an irregular shape and edges. All of

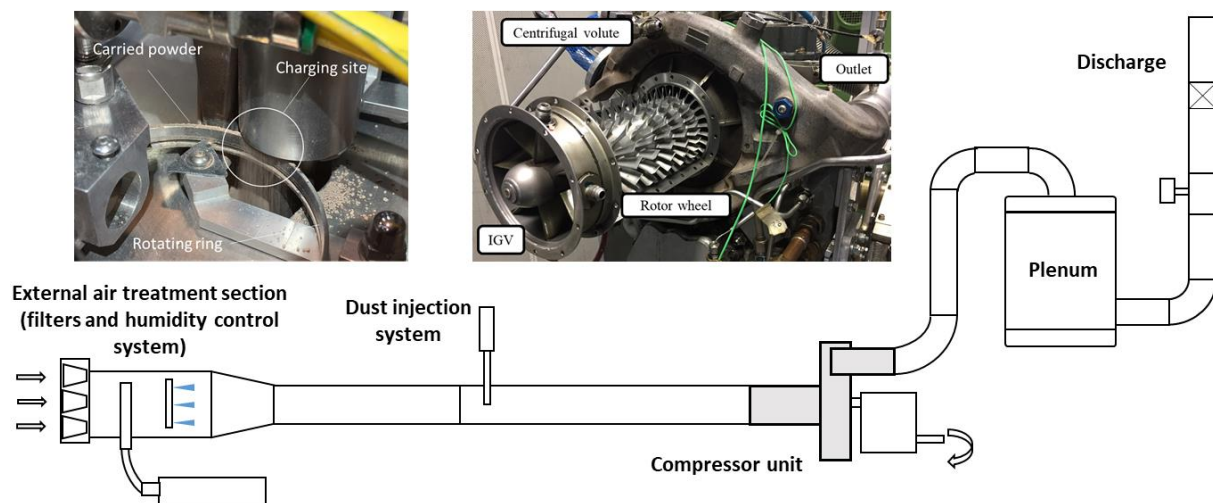


Figure 1. Test bench

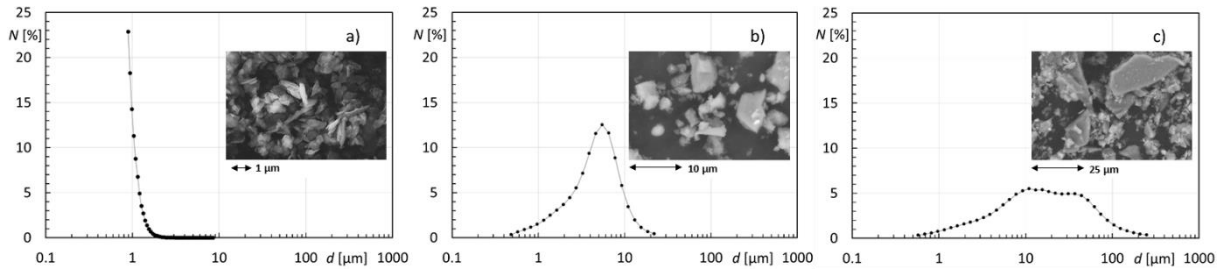


Figure 2. Particle diameter distributions: a) ARD N, b) ARD UF, and c) ARD M

the powder samples are provided by Powder Tech Inc. (Powder Technology Inc., Arden Hills, USA).

Image and deposit detections. To detect the deposits on the compressor blade and vane surfaces, a set of images of the compressor flow path has been taken during the experimental investigation. A proper light and camera setup was adopted to ensure the repeatability of the detection process, allowing the comparison between the clean and fouled blade according to the different powder size distributions. The image detection was carried out by disassembling the compressor unit. Thanks to this, the half compressor case (stator) was positioned on a realized-on-purpose holder while the rotor was kept in the original position. Since the rotor was detected without any disassembling procedure, the camera and light setup are installed directly on the rotating test rig (see Fig. 3). This fact implies several difficulties related to the proper detection of the flow path, mainly due to the thermal expansion of the compressor unit. Due to the lab-test conditions and the compressor geometry, the effects of the thermal expansion expire after five hours.

The deposit patterns are taken directly from the lab-testing facility employing dedicated cameras with a resolution of 3264 x 2448 pixels positioned to detect the entire flow path of the axial compressor divided according to the rotor and stator components. The white light setup is adopted for both parts of the compressor flow path with the intensity of 4000 K. In Fig. 3, the light setup for rotor and stator surfaces has been reported.

After the picture collection (clean and fouled conditions), the deposit patterns were determined through image processing based on the open-source package Image J [19] developed by the U.S. National Institutes of Health. The procedure [20 – 22] is based on subtracting the picture of the fouled surfaces and the picture of the clean one converting the resultant image into a binary format. Finally, the picture is converted to show the deposits as the grayscale-colored pattern on the picture. The procedure is summarized in Fig. 4.

Test matrix. To prove the capability of the measurement strategy to detect the fouled regions, a specific test matrix has been done. Since the adhesion process is strongly related to the combination between particle diameter and air humidity, the proposed analysis covers a humidity

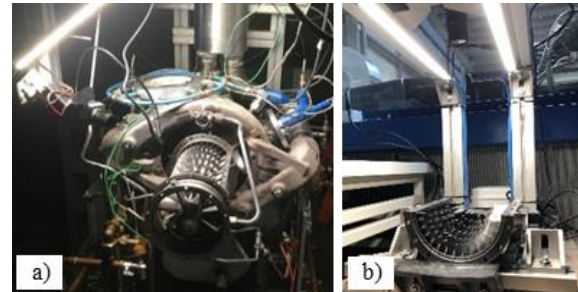


Figure 3. Light and camera setup for a) rotor and b) stator surfaces

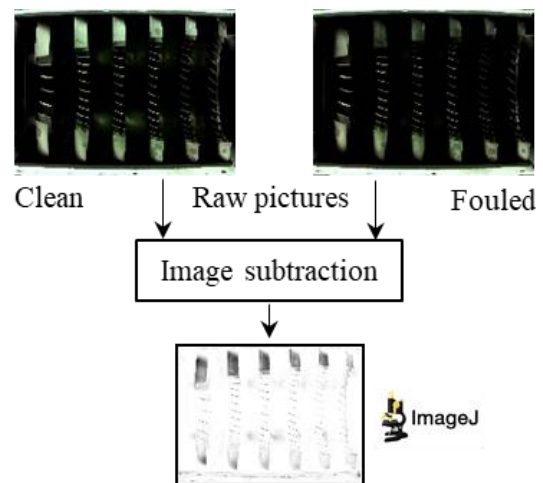


Figure 4. Strategy for the image post process

range of (15 – 80) %RH. Table 1 shows the tested conditions. The fouling tests cover the upper half-plane of the overall design. Each test had a duration of 4 hours. The powder concentration was kept constant and equal to 6 mg/m³ for all the tested powder by adjusting the ring speed of the feeder (see Fig. 1 for more details).

To ensure the repeatability of the results, at the beginning of each test, the compressor was deeply cleaned. The off-line cleaning has been done by disassembling the stator axial part to allow easy access to the rear stages of the compressor. The stator and rotor blades, the shroud, and the hub were

Table 1. Test matrix

	15 %RH	50 %RH	80 %RH
ARD N	×	-	×
ARD UF	-	×	×
ARD M	-	-	×

cleaned with demineralized water combined with a cleaner product and brushes to restore the initial condition of cleanliness. After the conclusion of the cleaning operation, pictures of the rotor and stator surfaces are taken. After the compressor start-up, the achievement of the desired operating point, and the assessment of the thermal equilibrium, the injection of the contaminant is carried out. The particle flow rate injected is kept constant for all the test duration. At the end of each test, the axial part is disassembled, and fouled pictures are taken.

RESULTS

The results of the present investigation are organized as follows. In the first part, an overview of detections is proposed to show the capability of this measurement process to detect different deposition patterns on compressor rotor and vanes surfaces. In the second part, a quantitative analysis has been proposed based on the image post-process. Finally, an assessment of the image analysis capabilities has been presented.

Image detections. Samples of image detections are proposed in Figs 5 – 7. These figures report the results from the deposition tests of ARD N with 15 %RH, ARD UF with 50 %RH, and ARD M with 80 %RH, respectively. The set of image reports from left to right the clean, fouled, and post-processed detections. Concerning a single picture, the front stages are on the right, while the rear stages (axial compressor discharge section) are on the left.

Comparing the clean and fouled detections, it is possible to see the deposition process affecting the blade and vanes surfaces and the hub and shroud surfaces. Increasing the particle diameter, the adhesion process becomes less effective even with greater humidity. A greater deposition can be found in the pressure side of the rotor blade and stator vanes as well as in correspondence of the leading edge. From Figs 5 – 7 is clear that using only the detection, a detailed comparison between the clean condition and the fouled one is not straightforward. In addition, by changing the contaminants, the comparisons became impossible. Based on the subtraction process between "fouled" and "clean" images, the image post-process allows the proper comparison. As seen from the analysis, the image-post process emphasizes the deposits patterns, generating a black and white map useful to consider how different contaminants and operating conditions affect the compressor surfaces. As reported in [23 – 25], the effects of deposits on compressor performance change according to the location on the blade surfaces. For example, the contamination on the suction side of the stator vanes changes over the stage, and only by using the post-processed images has it been possible to quantify. The smallest powder (ARD N) affects all stages, ARD UF affects only the first three stages, while the coarsest powder (ARD M) affects the first two

stages with a thin and non-homogenous layer. Rotor detections are affected by the hub surface reflection due to a mirror-like surface finishing, determining the impossibility of defining the proper contamination of the rotor hub. In addition, the shadows due to the half-part of the stator that can not be dismounted increases the inaccuracy of the image detections. Looking at rotor surfaces, similar considerations can be made in terms of contamination. The coarse powder (ARD M) does not determine relevant deposits concerning the smaller powder. In addition, the rotor surface is subjected to the centrifugal force that could be responsible for the detachment process of the deposits over the compressor operation.

Quantitative analysis. Starting from the post-processed image, a quantitative analysis can be done. The black and white images allow the comparison of the dirty and clean areas on the compressor surface. Figure 8 reports the quantitative analysis of the ARD N test with low and high relative humidity values. The comparison is based on the pixel count of the post-processed images. According to the adopted calculation (see Fig. 4 for more details), black pixels represent the dirty regions while white pixels represent the clean regions. Therefore, comparing the number of white and black pixels and the total pixel, it is possible to estimate the fouled portion of the interested surface. In Fig. 8, four representative pressure sides of the stator vane surfaces have been considered. The regions of interest for each vane have been highlighted with red lines. In these regions, the ImageJ software made a pixel count, and the ratio between white pixels and black pixels to the total number of pixels has been reported in pie charts. The increased humidity values determine more detrimental conditions increasing the adhesion capability of particles. At the same time, looking at the pie charts, a quantitative explanation of the deposits modification over the compressor flow path can be done. Greater humidity determines the greatest contamination of the first stage and a progressive reduction of the deposits. By contrast, for the same operating condition and contaminants, but during a dry period, the compressor experiences more significant contamination on the rear stage instead of the first stage.

To increase the capability of the present post-process to give quantitative data, an evolution of this pixel comparison is reported in [26]. The black and white conversion generates a straightforward application of the pixel counting technique but it leads to inaccuracies related to the choice of the threshold. In [26], a frequency analysis of the greyscale pixels has been done to prove the efficiency of compressor cleaner in removing soot particles from the blade surface.

Comparison. The final step of the present investigation is the assessment of the validity of the

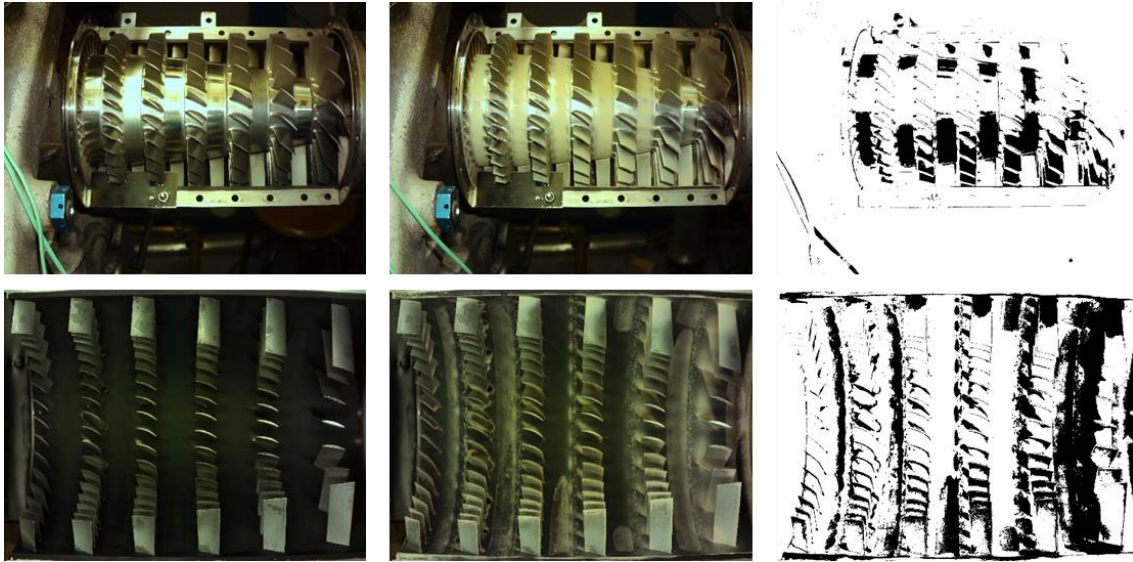


Figure 5. Detections (from left to right the clean, fouled, and post-processed images) for ARD N (15 %RH)

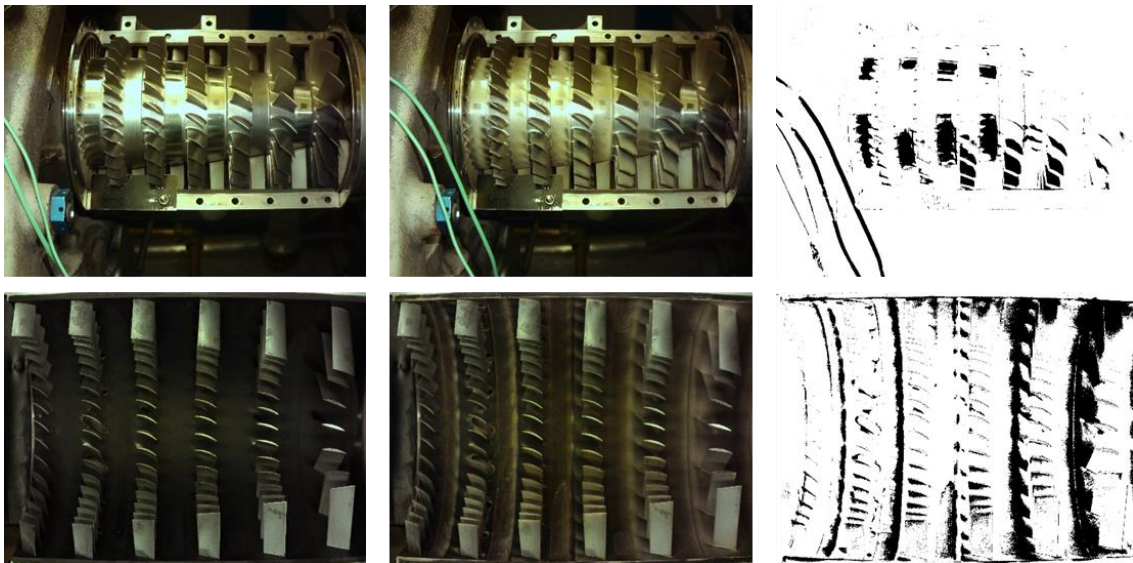


Figure 6. Detections (from left to right the clean, fouled, and post-processed images) for ARD UF (50 %RH)

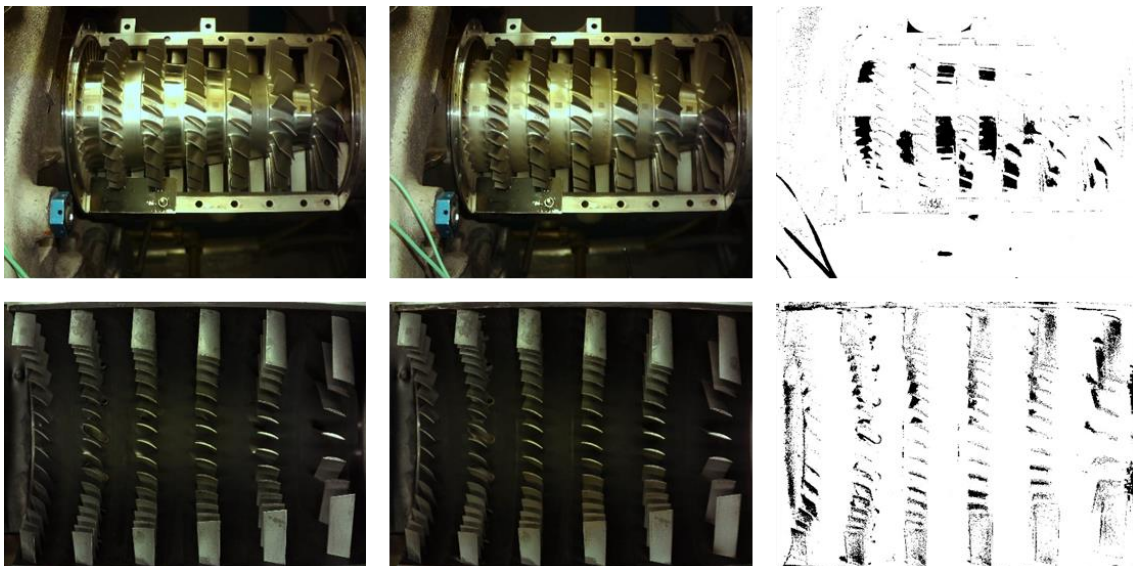


Figure 7. Detections (from left to right the clean, fouled, and post-processed images) for ARD M (80 %RH)

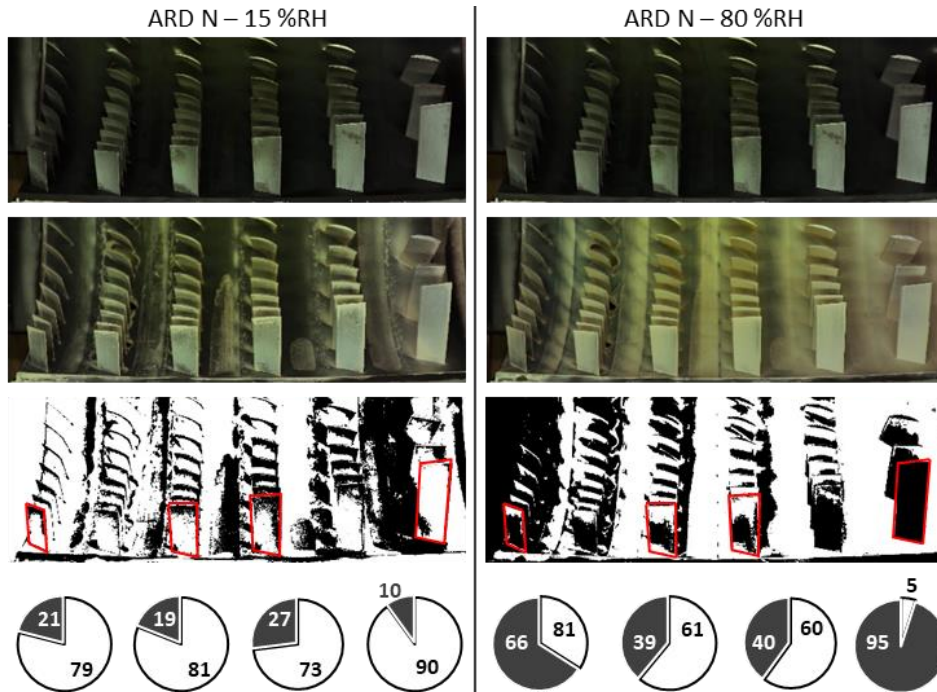


Figure 8. Sensitivity analysis to relative humidity for ARD N. The image analysis is dedicated to the pressure side of the stator vanes

image analysis. Since image detection could be very effective in the on-field application, using a lab-scale test, it is possible to define the reliability of the present procedure to represent a proper reference for future applications. To compare the image detection of the deposits (black and white pictures) with the actual intensity of the depots, a procedure reported in [27, 28] has been carried out. Therefore, the deposited dust on the compressor vanes has been measured employing an on-purpose designed device, the Localized Aspirator for Particle Observation (LAPO). The exploded view of the LAPO is depicted in Fig. 9. This device is a tool employed for particle sucking and measurement from surfaces driven by a vacuum pump. The system is based on a stainless steel needle with a diameter of 1 mm, which allows direct particle sucking from the surface of interest. In Fig. 9, the deposit collection from a stator vane leading edge is shown. The reported frames show the leading edge before and after the deposit collection, corresponding to the first passage time of the device. Depending on the stickiness of the deposited layer, a complete deposit

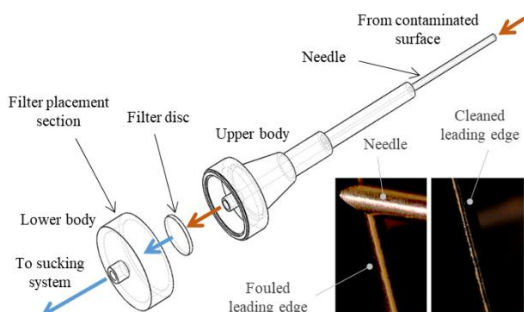


Figure 9. The LAPO system

removal can be achieved with multiple passages of the needle. The LAPO is equipped with a filter placement section allowing particle trapping and collection. At the end of the particle collection, the device is unscrewed, and the filter is removed and weighted to calculate the collected powder amount.

Figure 10 reports the mass of the deposits collected in correspondence to the pressure side of the stator vane surfaces. These quantitative measurements correspond to the same surfaces evaluated in Fig. 8. Comparing the analysis carried out by counting the pixel ratio and the collected mass, it can be concluded that the proposed measurement strategy allows an evaluation of the fouling phenomenon over the machine flow path. As can be seen from Fig. 10, front stages resulting from the high-humidity test are characterized by greater contaminant mass, similar to the results shown in Fig. 8. Image detection reveals the fouled area, and for this reason, comparing the deposited mass, some discrepancies could be detected. Looking at the aft stages, the deposited mass indicates that the relative humidity value does not affect the deposition process. By contrast, the image detection shows greater contamination for the test with 80 % RH. In the image detection, the deposited thickness is not detected, and a complete assessment of the deposited mass (i.e., volume) can not be assessed. The Shape From Shading (SFS) technique could represent a step forward in this sense. The SFS allows the obtainment of three-dimensional information starting from a two-dimensional detection. As shown in [29], this technique could be useful to estimate the deposits thickness even if, due to the mathematical constraints, the results have to

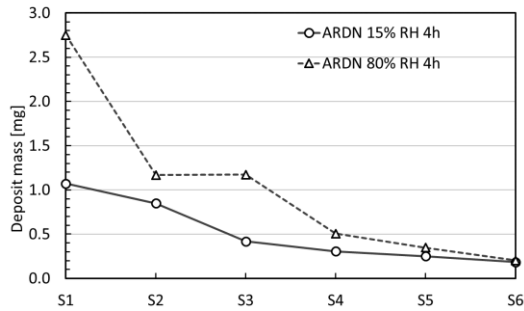


Figure 10. Mass deposits collected from the pressure side of the stator vanes

be validated after a calibration procedure, reducing the applicability to on-field detection.

Remarks and guidelines. According to the results, it can be highlighted that image detection allows the recognition of the fouled region over the compressor flow path. The capability of the image analysis to detect the modification of the compressor surface is based on the proper light and camera setup and is easy to be assessed. Since the image detection can be quickly done on-field, during an inspection and/or overhaul, in this last section, some guidelines have been reported to make this technique affordable and applicable. The comparison between fouled (or damaged) sections and the clean (or restored) ones can be made by acquiring the proper set of images immediately before and after the restoration process. In this way, qualified operators can realize the image detection within the maintenance intervals and compare the surface deterioration with the data coming from the control system of the unit, putting the basis to increase the comprehension of the unit operation. To do this, some hints are reported in the following:

- install the cameras in a fixed position, excluding vibration and lens deterioration (dirty or powder due to operation on the construction site);
- use artificial light setup (make the photographic set overnight), paying attention to the light intensity (sometimes the light intensity change due to voltage variation) and position (use the same light position before and after the restoring operations);
- detect several images from different perspectives. In this case, use multiple cameras to avoid the mount and dismount processes;
- use reference criteria (for example, a frame or fixed support) to have a fixed helpful point to compare the image and establish if the camera was moved or not;
- use a holding system to keep the compressor shaft in the same position before and after the overhaul process;
- cool down the unit, and remember that the thermal expansion could also be responsible for the deviation between clean and fouled conditions.

As shown in the previous paragraph, this technique is helpful in making a qualitative assessment of the contamination. A more precise detection to move this analysis from a qualitative to a quantitative framework should be based on the analysis of the shading (SFS techniques) and the possibility of checking the image detection with other possibilities based on the quantitative assessment of the deposited layer.

CONCLUSIONS

In the present investigation, the capability of the image detection to show a fouled pattern on an axial compressor unit has been proposed. Furthermore, a proper test bench has been developed to prove this fascinating measurement technique's capability. The test bench is based on an axial compressor, fouled with three different powders during the operation with three different relative humidity levels.

The analysis shows the capability of image detection to grasp the modification of the internal surface of the compressor as a function of the contamination process, leading to more detrimental conditions with smaller powder and greater humidity levels. Using an open-source software tool, the contamination has been quantified, starting from a simple image comparison. Estimating the percentage area of each blade and vane surface covered by the contaminants has shown that the image detection could represent valid support to detect the effects of fouling on compressor degradation. Finally, an estimation of the inaccuracy of the image detection method has been proposed showing that, in the case of non-uniform layer thickness, the analysis of the fouled area does not match with the estimation of the contaminant mass.

From the present results, it can be concluded that the image detection and post-process could be helpful in detecting the effects of compressor operation in harsh environments and make a reference during the overhaul operation of land based-unit. Furthermore, if applied systematically, this method could be used to feed a helpful database to correlate the machine operation with on-filed data and performance. A set of guidelines and key points were also listed to do this.

ACKNOWLEDGMENTS

The authors wish to thank Eng. Luca Panetto for its valuable support for carrying out the tests and the data post-process.

REFERENCES

- [1] Dahl, G., and Suttrop, F. Engine control and lowNOx combustion for hydrogen fuelled aircraft gas turbines (1998) International Journal of Hydrogen Energy, 23(8), pp. 695–704. DOI: 10.1016/S0360-3199(97)00115-8
- [2] Palies, P. P., Hydrogen thermal-powered aircraft combustion and propulsion system (2022)

- Proceedings of the ASME Turbo Expo - GT2022-78214
- [3] Kurz, R., Brun, K. Fouling mechanisms in axial compressors (2012) *Journal of Engineering for Gas Turbines and Power*, 134 (3), art. no. 032401. DOI: 10.1115/1.4004403
- [4] Diakunchak, I.S. Performance deterioration in industrial gas turbines (1992) *Journal of Engineering for Gas Turbines and Power*, 114 (2), pp. 161-168. DOI: 10.1115/1.2906565
- [5] Suman A., Morini M., Aldi N., Casari N., Pinelli M., Spina P.R. A compressor fouling review based on an historical survey of asme turbo expo papers (2017) *Journal of Turbomachinery*, 139 (4), art. no. 041005. DOI: 10.1115/1.4035070
- [6] Suman, A., Casari, N., Fabbri, E., di Mare, L., Montomoli, F., Pinelli, M. Generalization of particle impact behavior in gas turbine via non-dimensional grouping (2019) *Progress in Energy and Combustion Science*, 74, pp. 103-151. DOI: 10.1016/j.peccs.2019.05.001
- [7] Vulpio, A., Suman, A., Casari, N., Pinelli, M., Kurz, R., Brun, K. Analysis of Timewise Compressor Fouling Phenomenon on a Multistage Test Compressor: Performance Losses and Particle Adhesion (2021) *Journal of Engineering for Gas Turbines and Power*, 143 (8), art. no. 081005, DOI: 10.1115/1.4049505
- [8] Suman, A., Vulpio, A., Casari, N., Pinelli, M. Outstretching population growth theory towards surface contamination (2021) *Powder Technology*, 394, pp. 597-607. DOI: 10.1016/j.powtec.2021.08.071
- [9] Brun, K., Grimley, T.A., Foiles, W.C., Kurz, R. Experimental Evaluation of the Effectiveness of Online Water-Washing in Gas Turbine Compressors (2015) *Journal of Engineering for Gas Turbines and Power*, 137 (4), art. no. 042605. DOI: 10.1115/1.40286185
- [10] Casari, N., Pinelli, M., Spina, P.R., Suman, A., Vulpio, A. Performance degradation due to fouling and recovery after washing in a multistage test compressor (2021) *Journal of Engineering for Gas Turbines and Power*, 143 (3), art. no. 031020, DOI: 10.1115/1.4049765
- [11] Mund, F. C., and Pilidis, P. A review of gas turbine online washing systems (2004) *Proceeding of the ASME Turbo Expo - GT2004-53224*
- [12] Asplund, P. Gas turbine cleaning upgrade (compressor wash) (1997) In *Turbo Expo: Power for Land, Sea, and Air*, Vol. 78675, American Society of Mechanical Engineers, p. V001T09A003
- [13] Perullo, C.A., Lieuwen, T., Barron, J., Grace, D., Angello, L. Evaluation of air filtration options for an industrial gas turbine. (2015) *Proceedings of the ASME Turbo Expo*, 3, DOI: 10.1115/GT2015-43736
- [14] Meher-Homji, C.B., Chaker, M., Bromley, A.F. The fouling of axial flow compressors - Causes, effects, susceptibility and sensitivity. (2009) *Proceedings of the ASME Turbo Expo*, 4, pp. 571-590, DOI: 10.1115/GT2009-59239
- [15] Munari, E., Morini, M., Pinelli, M., Spina, P.R., Suman, A. Experimental Investigation of Stall and Surge in a Multistage Compressor (2017) *Journal of Engineering for Gas Turbines and Power*, 139 (2), art. no. 022605. DOI: 10.1115/1.4034239
- [16] Suman, A., Vulpio, A., Fortini, A., Fabbri, E., Casari, N., Merlin, M., Pinelli, M. Experimental analysis of micro-sized particles time-wise adhesion: the influence of impact velocity and surface roughness (2021) *International Journal of Heat and Mass Transfer*, 165, art. no. 120632, DOI: 10.1016/j.ijheatmasstransfer.2020.120632
- [17] Gómez-Moreno, F.J., Pujadas, M., Plaza, J., Rodríguez-Maroto, J.J., Martínez-Lozano, P., Artiñano, B. Influence of seasonal factors on the atmospheric particle number concentration and size distribution in Madrid (2011) *Atmospheric Environment*, 45 (18), pp. 3169-3180. DOI: 10.1016/j.atmosenv.2011.02.041
- [18] Wang, G.H., Zhou, B.H., Cheng, C.L., Cao, J.J., Li, J.J., Meng, J.J., Tao, J., Zhang, R.J., Fu, P.Q. Impact of Gobi desert dust on aerosol chemistry of Xi'an, inland China during spring 2009: Differences in composition and size distribution between the urban ground surface and the mountain atmosphere (2013) *Atmospheric Chemistry and Physics*, 13 (2), pp. 819-835. DOI: 10.5194/acp-13-819-2013
- [19] Schneider, C.A., Rasband, W.S., Eliceiri, K.W. NIH Image to ImageJ: 25 years of image analysis (2012) *Nature Methods*, 9 (7), pp. 671-675. DOI: 10.1038/nmeth.2089
- [20] Suman, A., Vulpio, A., Casari, N., Pinelli, M., Kurz, R., Brun, K. Deposition Pattern Analysis on a Fouled Multistage Test Compressor (2021) *Journal of Engineering for Gas Turbines and Power*, 143 (8), art. no. 081006, DOI: 10.1115/1.4049510
- [21] Casari, N.; Pinelli, M.; Suman, A.; Vulpio, A.; Appleby, C.; Kyte, S. Assessment of the washing effectiveness of on-purpose designed eco-friendly cleaner against soot deposits. *J. Glob. Power Propuls. Soc.* 2020, 4, 253–263
- [22] Casari, N., Pinelli, M., Suman, A., Vulpio, A. Performance losses and washing recovery of a helicopter engine compressor operating in ground-idle conditions (2022) *CEAS Aeronautical Journal*, 13 (1), pp. 113-125. DOI: 10.1007/s13272-021-00563-1
- [23] Morini, M., Pinelli, M., Spina, P.R., Venturini, M. Computational fluid dynamics simulation of fouling on axial compressor stages (2010) *Journal of Engineering for Gas Turbines and Power*, 132 (7), art. no. 072401. DOI:

- 10.1115/1.4000128
- [24] Morini, M., Pinelli, M., Spina, P.R., Venturini, M. Numerical analysis of the effects of non-uniform surface roughness on compressor stage performance (2011) *Journal of Engineering for Gas Turbines and Power*, 133 (7), art. no. 072402. DOI: 10.1115/1.4002350
- [25] Aldi, N., Morini, M., Pinelli, M., Spina, P.R., Suman, A., Venturini, M. Performance evaluation of nonuniformly fouled axial compressor stages by means of computational fluid dynamics analyses (2013) *Journal of Turbomachinery*, 136 (2), art. no. 021016. DOI: 10.1115/1.4025227
- [26] Vulpio, A., Suman, A., Casari, N., Pinelli, M., Appleby, C., Kyte, S. Washing effectiveness assessment of different cleaners on a small-scale multistage compressor (2021) *Proceedings of the ASME Turbo Expo*, 8, art. no. V008T20A013. DOI: 10.1115/GT2021-59455
- [27] Vulpio, A., Suman, A., Casari, N., Pinelli, M. A Simplified Method for the Deposition Rate Assessment on the Vanes of a Multistage Axial-Flow Compressor (2022) *Journal of Turbomachinery*, 144 (7), art. no. 71009. DOI: 10.1115/1.4053288
- [28] Vulpio, A., Suman, A., Casari, N., Pinelli, M. Dust ingestion in a rotorcraft engine compressor: Experimental and numerical study of the fouling rate (2021) *Aerospace*, 8 (3), art. no. 81. DOI: 10.3390/aerospace8030081
- [29] Casari, N., Fortini, A., Pinelli, M., Suman, A., Vulpio, A., Zanini, N. Measurement approaches for the analysis of soil layer by microparticle adhesion (2022) *Measurement: Journal of the International Measurement Confederation*, 187, art. no. 110185, DOI: 10.1016/j.measurement.2021.110185